SEMARAK ILMU PUBLISHING

Journal of Advanced Research in Numerical Heat Transfer

Journal homepage:
https://semarakilmu.com.my/journals/index.php/arnht/index
ISSN: 2735-0142

Numerical Analysis of Battery Thermal Management System of Electric Vehicle

Lai Qit Inn[1,*], A. N. Oumer[2], Azizuddin Abd Aziz[1], Januar Parlaungan Siregar[2], Tezara Cionita[3]

[1] Faculty of Mechanical & Automotive Engineering Technology (FTKMA), Universiti Malaysia Pahang, 26600 Pekan, Pahang, Malaysia
[2] College of Engineering (KKEJ), Universiti Malaysia Pahang, 26600 Pekan, Pahang, Malaysia
[3] Department of Mechanical Engineering, Faculty of Engineering and Quantity Surveying, INTI International University, 71800 Nilai, Negeri Sembilan, Malaysia

ARTICLE INFO

Article history:
Received 9 March 2023
Received in revised form 22 April 2023
Accepted 16 May 2023
Available online 30 June 2023

Keywords:
BTMS; heat transfer coefficient; pressure difference; ANSYS; MINITAB

ABSTRACT

This study is modelling the direct liquid cooling system of battery used in Electric Vehicle. The purpose of the study is to investigate the performance of the Li-ion battery model under different input of parameters and to evaluate the optimum parameters for the battery thermal management system model to maintain at its peak performance. SolidWorks and ANSYS are used to model and simulate the battery whereas MINITAB software is selected for conducting the statistical analysis. Heat flux, mass flow rate at the inlet and the thickness of the battery model has been selected as input of the simulation. The obtained results show that the heat transfer coefficient is increasing with the higher heat flux and mass flowrate but decreasing with the thickness of the battery model. Pressure drop remains constant when heat flux varies but increasing with mass flow rate and inversely proportional with the thickness of battery. For statistical analysis, an optimum value for the parameters is proposed to maintain the battery to operate with a highest heat transfer coefficient but lowest in pressure difference. Overall, the study has been conducted successfully and fulfilled the objectives stated.

1. Introduction

Electric Vehicle (EV) is gaining popularity in automotive industry recent years and mostly is due to the price of oil rises rapidly internationally. Therefore, people will be more willing to choose EV as an alternate of transportation as compare with conventional internal combustion engine as fuel is a non-renewable source and eventually will be used up at the end of the day. Besides, fueling with electricity is more environment-friendly and it helps to reduce the harm towards the mother nature. EV which uses electricity to power itself, will not produce any smog or exhaust that will pollute the city that leads to greenhouse effect [1]. The battery in EV can be charged by plugging in via the charging port or through recuperation during braking. The electricity charged will be stored in the battery pack while motor controller will supply varying power to the electric motor. The electric

* *Corresponding author.*
E-mail address: laiqitinn@gmail.com (Lai Qit Inn)

https://doi.org/10.37934/arnht.13.1.106114

motor will then convert the electricity into mechanical energy and when used within a drivetrain to torque [2]. Moreover, the battery pack powers to motor controller which in turn delivers it to the electric motor. When the pedal receives a pair of potentiometers that activate the motor controller to power the electric motor therefore when the car is stationary, the controller will not deliver any power to the electric motor [3]. Battery is the crucial part in EV hence the success of the EV is basically dependent on the battery development. Under the wider charging and discharging condition with high level of current input, EV gains power source from the battery and the battery will generate and accumulates a lot of heat. There are some battery types which are suitable to use in EV: Lithium-ion battery (Li-ion), Nickel metal hydride battery (NiMH), Lead- acid battery, Lithium polymer battery and Fuel cell technology [4]. In most case, to power an EV, battery cells will be arranged in different arrays to form a battery module. With knowing the desired capacity and voltage in advance, the battery modules will be merged into a battery pack for the EV.

2. Battery Thermal Management System

Srinivasan and Wang [5] mentioned that the heat generation in battery pack are from these aspects: heat generation from Joule Heating, heat generation from Electrode Reactions and Entropic heat generation. Therefore, the heat generated should be transferred to the surrounding efficiently so that the temperature inside the battery pack would not exceed the safety temperature range or else thermal runaway may occur in the battery pack [6]. The thermal runaway is caused by imbalance between the heat generated from the cell and heat dissipation from the battery pack. Thermal runaway in battery can lead to fire or in some severe case, explosion could happen. In order to maintain the battery temperature at an optimum range, Battery Thermal Management System (BTMS) is developed in the system. There are two categories for BTMSs: active and passive cooling system. In active cooling system, the total heat produced will be cooled down by medium like air or liquid whereas for passive cooling system, heat will be absorbed by the Phase Change Material (PCM) which is inserting in the battery pack. Chen *et al.,* [7] used CFD analysis to estimate the hot spots and cold spots within the battery pack. The outcome of the simulation shown that acceleration of the cooling air flowing in the battery pack increases the heat transfer coefficient and pressure drop as well. Saw *et al.,* [8] used Computation Fluid Dynamic (CFD) software, ANSYS-CFX to solve the flow field which is hard to be obtained in real-life experiments. Computer Aided Design model of the battery pack has been imported for meshing using ANSYS ICEM CFD 14.0 SP1. CFX solver is used to solve the equations of mass conservation, momentum conservation and energy conservation equation. Li *et al.,* [9] applied CFD software to solve the thermodynamic mathematical models of the system applying PCM.

The purpose of this study is to investigate the performance of the Li-ion battery model under different input of parameters and to evaluate the optimum parameters for the battery thermal management system model to maintain at its peak performance. SolidWorks and ANSYS are used to model and simulate the battery whereas MINITAB software is selected for conducting the statistical analysis.

3. Methodology

3.1 Simulation

In this project, the battery model is built according to the 21700 Li-ion battery cells with diameter of 21mm and height of 70mm. The battery module consists of total 96 cylindrical. Considering the complexity to complete the simulation in software, some assumptions are made to simplify the

simulation process. As the internal structure of a real battery cell is complex and therefore will be neglected and the battery will be assumed to be a constant heat source. Therefore, in this project only considering the one of the cross-sectional areas of the battery module as shown in Figure 1. The details of the material properties are shown in Table 1.

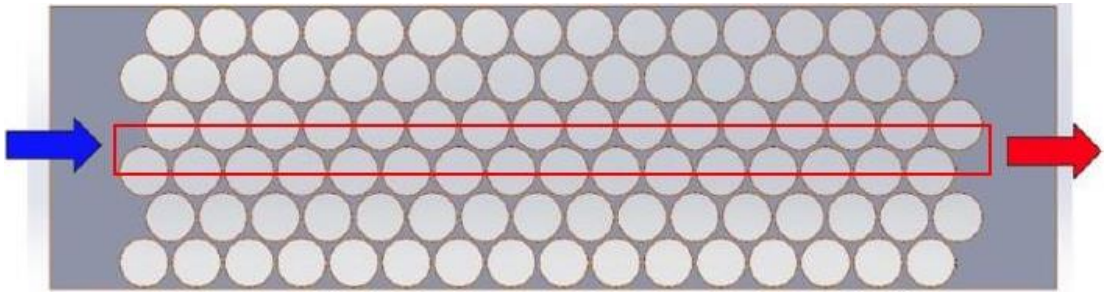

Fig. 1. The cross-sectional area considering for the battery module

Table 1
The properties of the material

Materials	Density ($\boldsymbol{kg/m^3}$)	Specific heat ($\boldsymbol{J/\ kgK}$)	Viscosity ($\boldsymbol{kg/ms}$)	Thermal conductivity ($\boldsymbol{W/mK}$)
Fluid				
3M Novec	1660	1130	0.00087	0.06
Solid				
Polypropelene	905	1571	-	0.22

In the boundary conditions setting, the initial fluid mass flow rate at the inlet is set to be 0.0746 kg/s while the inlet temperature is set to be 293 K. Pressure outlet is selected at the outlet and equals to the atmospheric pressure. The data was employed from Moghaddam [10]. Top surface, bottom surface and tubes surfaces are all set as stationary wall and no slip for the shear condition. Thermal condition at the tubes surface selects heat flux as the data input by employing (1. The surface area of a 21700-battery cell is calculated as $5.31x10^{-3}m^2$ and the heat generation per cell ($4.4W$) is obtained from the present study.

$$Heat\ flux = \frac{Heat\ generation\ per\ cell}{Surface\ area\ of\ battery} \tag{1}$$

Moreover, turbulent model is selected as the model in the simulation by calculating the Reynold's number (Re) using (2 where ρf is the fluid density (1660 kg/m^3), v is the fluid velocity, L indicates the characteristics length of the fluid flow (0.0460m) while μf is the dynamic viscosity of the fluid (0.00087kg/ms). The Re calculated is 2300 and the flow is designed as laminar flow.

$$Re = \frac{\rho_f v L}{\mu_f} \tag{2}$$

Heat flux, which denoted by q, generated from the battery cell can be defined as the heat generated from the battery cell per unit surface area as shown in Eq. (3). As the surface area of the heat transfer in the simulation model will be kept constant, the heat generated by the cell is directly proportional to the heat transfer coefficient, indicating that increasing of the amount of heat generated from the battery cell will rise the heat transfer coefficient and eventually perform a higher efficiency of heat transfer. The mean of the fluid temperature is the average of the fluid temperature at both inlet and outlet as shown in Eq. (4). Despite of the heat flux and mass flow rate, geometrical

parameter is also taken in consideration to study the effect of heat transfer of the model. Initially, the distance between each roll of the battery cell is set as 24.5mm as shown in Figure 2. The model is rebuilt by narrowing and widening the distance. As the distance varies, the area for the fluid to flow through changing too. This applies to the pressure difference at the inlet and outlet as well. The tolerance of the thickness is 1mm varying from 21.5mm to 27.5mm.

$$q = \frac{Q}{A} = h\left(T_{wall} - T_{fluid}\right) \tag{3}$$

$$T_{fluid} = \frac{Temperature_{inlet} + Temperature_{outlet}}{2} \tag{4}$$

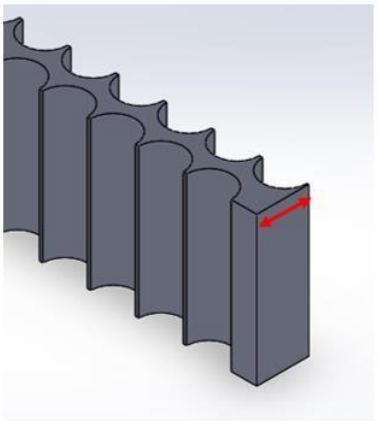

Fig. 2. The distance between each row of the battery cell

Both inlet and outlet temperature will be taking the average temperature and divided by 2. The tubes surface temperature which also known as the wall temperature, will be collected in average value as well.

$$Mean\ temperature = \frac{T_{in,avg} + T_{out,avg}}{2} \tag{5}$$

Eq. (6) is applied to calculate the heat transfer coefficient by varying heat flux, mass flow rate and the geometry of the model. When one of the parameters is being studies, the rest of the parameters will be kept constant to evaluate the most accurate results.

$$h = \frac{q}{T_{wall,avg} - T_{mean}} \tag{6}$$

4. Statistical Analysis

To achieve the second objective, which is to determine the most optimum parameter for the battery module to perform at its highest efficiency, MINITAB software has been applied to carried out the statistical analysis on the data collected. From the previous section, three parameters are selected to manipulate and observe the battery performance (see Table 2). By creating a new Central Composite design in MINITAB, the order generated are then simulated in ANSYS again. The responses of the design are denoted by h and $deltp$ which represents heat transfer coefficient and pressure difference, respectively (see Figure 3).

Table 2
The settings in MINITAB

	Parameters	Symbols
Factors		
A	Heat flux	q
B	Mass flow rate	m
C	Thickness	t
Response	Heat transfer coefficient	h
	Pressure difference	deltp

C1	C2	C3	C4	C5	C6	C7	C8	C9
q	m	t	h	deltp	StdOrder	RunOrder	Blocks	PtType
476.42	0.0454	24.5	120.61	41.14	1	1	1	1
476.42	0.0454	24.5	120.61	41.14	2	2	1	1
830.19	0.0746	27.5	31.77	34.46	3	3	1	1
122.64	0.0162	27.5	24.73	2.35	4	4	1	1
830.19	0.0162	21.5	193.52	19.52	5	5	1	1
122.64	0.0746	21.5	59.25	367.21	6	6	1	1
830.19	0.0162	27.5	18.97	2.35	7	7	1	1
122.64	0.0746	27.5	59.10	40.46	8	8	1	1
122.64	0.0162	21.5	65.94	19.52	9	9	1	1
476.42	0.0454	24.5	120.61	41.14	10	10	1	1
830.19	0.0746	21.5	369.80	367.21	11	11	1	1
476.42	0.0454	24.5	120.61	41.14	12	12	1	1
476.42	0.0454	24.5	120.61	41.14	13	13	1	1
1054.13	0.0454	24.5	99.92	41.14	14	14	1	1
101.30	0.0454	24.5	51.52	41.81	15	15	1	1
476.42	0.0454	19.6	21.06	275.20	16	16	1	1
476.42	0.0454	24.5	120.61	41.14	17	17	1	1
476.42	0.0023	24.5	10.23	0.26	18	18	1	1
476.42	0.0454	29.4	25.46	11.19	19	19	1	1
476.42	0.0931	24.5	156.46	167.43	20	20	1	1

Fig. 3. The run order generated in MINITAB software

5. Results and Discussion

5.1 Heat Transfer

As a result, the variation of heat flux, mass flow rate and thickness with the heat transfer coefficient and pressure difference will be shown in graph. The value of heat flux is varying from 122.64 W/m^2 to 830.19 W/m^2. Any heat flux out of this range is not taken into consideration of the study because 0.65W of heat generated from the battery cell is equivalent to the heat dissipated from the cell under 1C of the charging or discharging rate. While 4.4W of the heat generated from the cell will be reaching the cooling limit of the coolant.

As shown in Figure 4(a), the heat flux applied at the tubes surface is increasing from 122.64 W/m^2 to 830.19 W/m^2 and the value of heat transfer coefficient increasing gradually with the heat flux applied as well. This is because when the battery module is operating, the cell will dissipate heat to the fluid. As more heat is generated, the coolant plays a role to transfer the heat from the heat source to the outlet. Since more heat is dissipating from the heat source, the higher value of the heat transfer coefficient also indicates a higher rate of heat transfer. As mentioned in the present study, the maximum temperature difference for the coolant to perform at its best efficiency must not exceed 5℃. In this section, the temperature difference resulted in all the ranges of heat flux is maintained within 1℃ to 2℃. As shown in Figure 4(b), the value of heat transfer coefficient increases consistently when mass flow rate increase from 0.0162 kg/s to 0.0746 kg/s. Under a constant surface area and

density of fluid, a higher rate of mass flow in a constant time indicates that letting more mass of fluid passing though the model. As more particles are flowing in the fluid, the velocity will increase and elevate the rate of convective at the same time. As a result, heat dissipated from the battery will be transferred to the fluid more effectively and eventually cool down the battery temperature. With this, it can be concluded as the higher the mass flow rate of the fluid, the higher the value of heat transfer coefficient and a higher rate of heat transfer. From the trendline plotted in the graph, it can be clearly seen that the overall trend of the variation of heat transfer coefficient and thickness is decreasing when the value of thickness is getting larger. This is because when the distance between each row of the battery cell is getting nearer, the surface area for the fluid to pass through from inlet to the outlet of the model is getting smaller too. When the mass flow rate and the density of the fluid remain constant, the velocity of the flowing fluid will increase hence increasing the rate of heat transfer in the model as well.

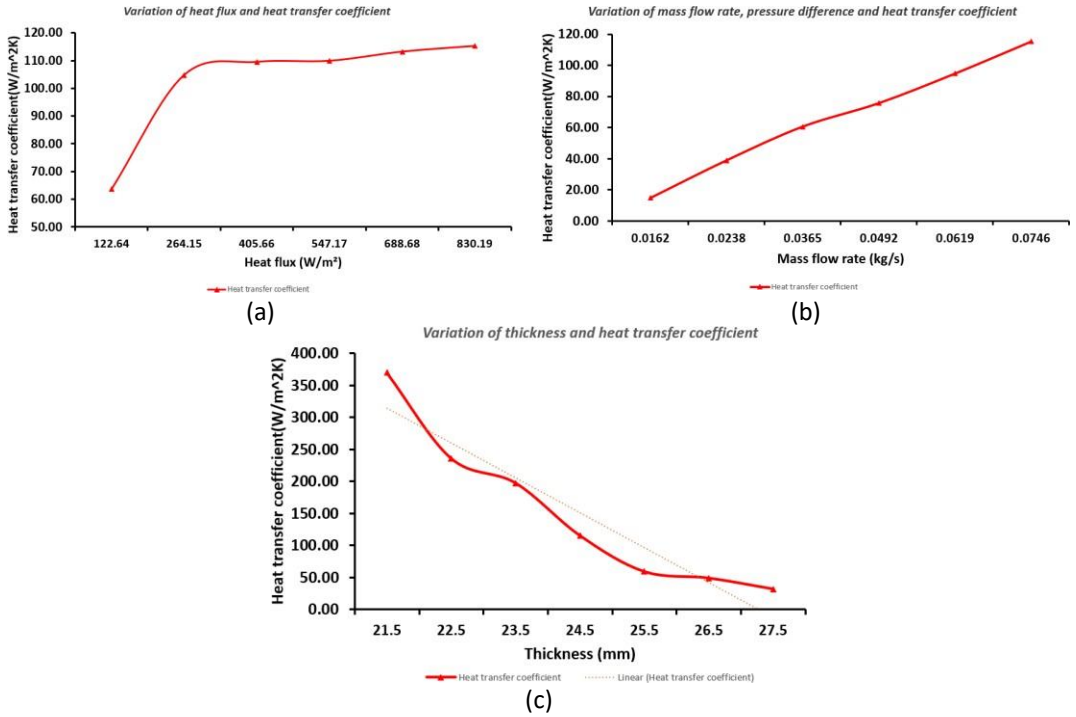

Fig. 4. Variation of heat transfer coefficient (a) with heat flux; (b) mass flow rate; (c) with thickness

5.2 Flow Performance

In this section, the flow performance obtained from the previous parameter will be discussed by observing the pressure drop of the model. Pressure difference is imported to studied in this simulation as the greater the pressure difference in the model indicated that more energy needs to be pumped from the inlet to the outlet of the model to achieve the heat transfer effect. When applying different values of heat flux on the tubes surface, the velocity of the fluid and surface area for the fluid to pass through is remained constant. Therefore, the pressure difference will be remained unchanged as well. Increasing in mass flow rate is allowing a greater number of particles to flow through a constant area per unit time. As more mass of particles is flowing through the constant surface area, there will be higher pressure resulted at the model. From Figure 5(c), the variation of the pressure difference shows a downtrend when the thickness of the model is increasing. The model with 24.5 mm of thickness resulted a 367.21 Pa of pressure drop whereas

model with 27 mm of thickness generated a pressure drop of 34.46 Pa. When the distance between the row of the battery increases, the surface area for the fluid to flow through increases. As pressure is inversely proportional with area, the increasing of area indicates the dropping of pressure in the model.

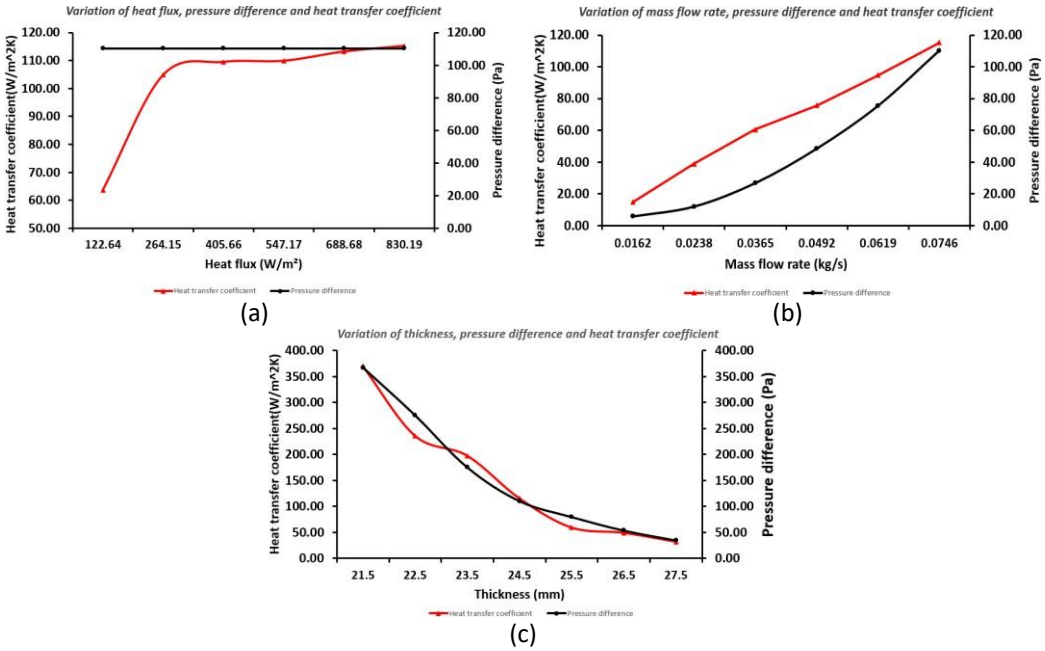

Fig. 5. Variation of pressure difference (a) with heat flux; (b) with mass flow rate; (c) thickness

5.3 Statistical Analysis

The response optimizer helps to design an optimal setting according to the factors selected. From the parameter table, the aim is to obtain a minimum pressure difference whereas a maximum for heat transfer coefficient. Therefore, a value of 0.262Pa is the best result while value exceeds 367.21Pa are not acceptable. For heat transfer coefficient, the ideal value is 369.80W/m^2K but values lower than 10.23 W/m^2 are not acceptable. The weight and importance columns indicate that both parameters have the same importance value as well as influence the composite desirability equally (see Figure 6). The multiple response prediction shows the range of the likely range for each response. It shows that an ideal result could be obtained by applying a value for heat flux at 1054.13 W/m^2, mass flow rate of 0.0142 kg/s and thickness of 20.69 mm. The mean pressure difference is 54.3Pa and the range of likely value is between -44.4Pa to 153.0Pa. Since the pressure difference should always positive, any values smaller than 0Pa can be neglected. The mean heat transfer coefficient is 201.2 W/m^2K and the range of likely value lies between −26.1 W/m^2K and 428.5 W/m^2K (see Figure 7). However, the value of heat transfer coefficient should always greater than zero thus any value smaller than zero can be ignored and narrowed the range to get a more precise results and increase the data accuracy.

Parameters

Response	Goal	Lower	Target	Upper	Weight	Importance
deltp	Minimum		0.262	367.210	1	1
h	Maximum	10.2345	369.795		1	1

Fig. 6. Parameter table in response optimizer

Multiple Response Prediction

Variable	Setting
q	1054.13
m	0.0142068
t	20.6897

Response	Fit	SE Fit	95% CI	95% PI
deltp	54.3	36.3	(-26.6, 135.2)	(-44.4, 153.0)
h	201.2	83.6	(14.9, 387.5)	(-26.1, 428.5)

Fig. 7. Multiple response prediction result in response optimizer

From the optimization plot shown in Figure 8, it will show the fitted values for the predictor setting. For the pressure difference, the goal is to minimize it and the composite desirability is 0.6730. Composite desirability is a weighted mean of the individual desirability for the responses, and it can observe how well the parameters combination satisfy the goal set to be achieved. The current setting for the parameters is: heat flux = 1054.13 W/m^2K, mass flow rate 0.0142kg/s, thickness = 20.69 mm. The predicted outcome for pressure difference is 54.30Pa while its individual desirability is 0.53118. Increasing in value of heat flux increases the heat transfer coefficient but brings a small effect on pressure difference. Therefore, heat flux is suggested to be set to the highest value. Increasing in mass flow rate increases both the responses. Therefore, a lower medium range of value is selected (0.0142 kg/s) to achieve the lowest pressure difference and targeted heat transfer coefficient. Increasing in thickness will decrease the heat transfer coefficient while the pressure difference can be controlled at a lower value for a certain range of the thickness. Therefore, it is recommended to set the thickness at 20.69 mm because at this point maximum heat transfer coefficient can be achieved. Even though the thickness around 28 mm can achieve the minimum pressure difference too but it will reduce the performance of heat transfer coefficient hence it is suggested to set the thickness as 20.69 mm.

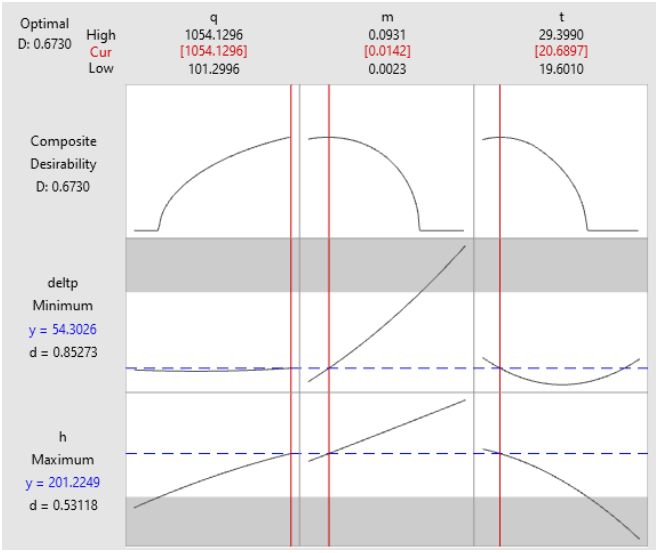

Fig. 8. Optimization plot from MINITAB

6. Conclusion

All in all, the objectives of the project have been achieved. Instead of simulating the entire model, the theory of simulating one of the sections from the model can generate the results which lies within an acceptable range. Besides, the maximum temperature difference of the inlet and outlet is maintained at the range of 6℃. To achieve a best heat transfer performance for the battery model, high heat flux applied on the wall surface with an optimum mass flow rate and a smaller distance between the successive row of batteries can be built. Besides, the model demonstrates that an ideal heat transfer ability with relatively low-pressure difference hence reducing the pump power as well as the energy consumption. In the statistical analysis, a suggested value for those three parameters is predicted to get the results with maximum heat transfer coefficient but minimum pressure difference. There are some recommendations to improve and enhance the current design. The mesh quality of the model can be enhanced by using a finer mesh for simulating a more accurate result. Besides, manipulation of different input parameters can be applied in the simulation software to observe the battery performance. For instances, change the inlet mass flow rate to inlet velocity or use different types of coolant as properties of fluid brings an impact on the results as well. Furthermore, it is suggested to build a prototype of the model so that the data collected can be validated and compared with the results obtained from simulation.

Acknowledgements
The authors are grateful to the University of Malaysia Pahang for providing the required support through the UMP Fundamental Research Grant scheme under project no. RDU190319.

References

[1] Un-Noor, Fuad, Sanjeevikumar Padmanaban, Lucian Mihet-Popa, Mohammad Nurunnabi Mollah, and Eklas Hossain. "A comprehensive study of key electric vehicle (EV) components, technologies, challenges, impacts, and future direction of development." *Energies* 10, no. 8 (2017): 1217. https://doi.org/10.3390/en10081217

[2] Helmers, Eckard, and Patrick Marx. "Electric cars: technical characteristics and environmental impacts." *Environmental Sciences Europe* 24, no. 1 (2012): 1-15. https://doi.org/10.1186/2190-4715-24-14

[3] Samara, S. "Electric Cars: Perception and Knowledge of the New Generation Towards Electric Cars." *Erasmus School of Economics* (2016).

[4] Palihawadana, Adeepa. "Electric Vehicle Battery Management System." *Master's thesis, University of Wolverhampton* (2016).

[5] Srinivasan, Venkat, and Chao-Yang Wang. "Analysis of electrochemical and thermal behavior of Li-ion cells." *Journal of The Electrochemical Society* 150, no. 1 (2002): A98. https://doi.org/10.1149/1.1526512

[6] Samba, Ahmadou. "Battery electrical vehicles-analysis of thermal modelling and thermal management." *PhD diss., LUSAC (Laboratoire Universitaire des Sciences Appliquées de Cherbourg), Université de caen Basse Normandie; MOBI (the Mobility, Logistics and Automotive Technology Research Centre), Vrije Universiteit Brussel*, 2015.

[7] Chen, Kai, Weixiong Wu, Fang Yuan, Lin Chen, and Shuangfeng Wang. "Cooling efficiency improvement of air-cooled battery thermal management system through designing the flow pattern." *Energy* 167 (2019): 781-790. https://doi.org/10.1016/j.energy.2018.11.011

[8] Saw, Lip Huat, Yonghuang Ye, Andrew AO Tay, Wen Tong Chong, Seng How Kuan, and Ming Chian Yew. "Computational fluid dynamic and thermal analysis of Lithium-ion battery pack with air cooling." *Applied Energy* 177 (2016): 783-792. https://doi.org/10.1016/j.apenergy.2016.05.122

[9] Li, Yantong, Yaxing Du, Tao Xu, Huijun Wu, Xiaoqing Zhou, Ziye Ling, and Zhengguo Zhang. "Optimization of thermal management system for Li-ion batteries using phase change material." *Applied Thermal Engineering* 131 (2018): 766-778. https://doi.org/10.1016/j.applthermaleng.2017.12.055

[10] Moghaddam, Seyed Mazyar Hosseini. "Designing battery thermal management systems (BTMS) for cylindrical Lithium-ion battery modules using CFD." *Master's thesis, KTH School of Industrial Engineering and Management* (2018).